INTERNATIONAL JOURNAL OF OPTIMIZATION IN CIVIL ENGINEERING
Int. J. Optim. Civil Eng., 2024; 14(1):139-161

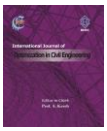

A METAHEURISTIC FRAMEWORK TO IMPROVE NONLINEAR FINITE ELEMENT ANALYSIS

A.H. Karimi[*, †], A. Bazrafshan Moghaddam
Department of Civil Engineering, Shahrood University of Technology, Shahrood, Iran

[DOI: 10.22068/ijoce.2024.14.1.579]

ABSTRACT

Most industrial-practical projects deal with nonlinearity phenomena. Therefore, it is vital to implement a nonlinear method to analyze their behavior. The Finite Element Method (FEM) is one of the most powerful and popular numerical methods for either linear or nonlinear analysis. Although this method is absolutely robust, it suffers from some drawbacks. One of them is convergency issues, especially in large deformation problems. Prevalent iterative methods such as the Newton-Raphson algorithm and its various modified versions cannot converge in certain problems including some cases such as snap-back or through-back. There are some appropriate methods to overcome this issue such as the arc-length method. However, these methods are difficult to implement. In this paper, a computational framework is presented based on meta-heuristic algorithms to improve nonlinear finite element analysis, especially in large deformation problems. The proposed method is verified via different benchmark problems solved by commercial software. Finally, the robustness of the proposed algorithm is discussed compared to the classic methods.

Keywords: Nonlinear analysis, finite element method, meta-heuristic algorithm, continuum mechanics, enriched firefly algorithm, large deformation, optimization.

Received: 21 November 2023; Accepted: 13 January 2024

1. INTRODUCTION

Most industrial-practical projects deal with nonlinearity phenomena. This is due to changes in linear assumptions in any part of force-stress, stress-strain, and strain displacement relations. The large deformation, material plasticity, and contact problems are the most famous problems in continuum mechanics that are categorized as nonlinear problems. A

[*]Corresponding author: Department of Civil Engineering, Shahrood University of Technology, P.O.Box 3619995161, Shahrood, Iran.
[†]E-mail address: amirhosseinkarimi@shahroodut.ac.ir (A.H. Karimi)

nonlinear analysis is required for solving a nonlinear problem. Among various analytical, experimental, and numerical methods, the Finite Element Method (FEM) is one of the most powerful and confident methods. It is possible to divide the FEM into three main Pre-Processing, Processing, and Post-Processing Steps. According to the nature of the nonlinear problems, their solving procedure is absolutely cost (Time and Memory) consuming. Therefore, to control the entire problem cost, it is possible to manipulate different parts of the FEM analysis [1].

In dealing with pre-processing step, it is possible to change the nodal numbering in order to reduce the bandwidth of the stiffness matrix and reduce the computational time [2–7]. Another efficient technique is to decompose the problem domain into the sub-domains and control the time and memory cost simultaneously [8–14]. Literature indicates that the mentioned procedure above decreases the time of the analysis impressive [15].

In the case of the processing step, one of the most challenging parts is solving the system of algebraic equations. This procedure can be optimized using mathematical or intelligent methods [16–20]. Another cost-consuming part of the FEM problems is the calculation of the stress fields. In the prevalent FEM, the main computational field is displacement and the other ones are obtained according to the nodal values of the displacement field. Therefore, it is vital to recovering any other fields, such as strain or stress, from nodal values. This procedure includes a high level of error and requires significant computations. This procedure also can be improved by Artificial Intelligence (AI) to reduce the allocated time and memory [21, 22]. The more complex problem, the more computational cost. Therefore, in complicated problems, such as those dealing with nature (soil, rock, contact, etc.,), AI methods can decrease the problem cost very effectively [23–28].

However, the most challenging step in the FEM analysis, especially in nonlinear problems, is to vanish residuals. Residuals are those variables that appear in the problem-solving procedure due to inaccuracy in the guessed fields according to the iterative behavior of the solver. A numerical solver should eliminate this residual in each step. Therefore, the power of the selected method as a solver is the most important part of the FEM analysis. It is shown that the prevalent solvers such as the Newton-Raphson method are not applicable in all nonlinear problems. Therefore, various modified versions of the Newton-Raphson method and the other gradient-based algorithms are developed. However, these modified versions are not accurate in all problems, and in some cases, similar to other alternative methods such as the Arc-Length method, are difficult to implement.

It seems that Artificial Intelligence (AI) as an appropriate, accurate, robust, and easy-to-implement approach, can help researchers to overcome the difficulties of the Nonlinear Finite Element Analysis. In this paper, a computational framework is presented based on meta-heuristic algorithms to improve nonlinear finite element analysis, especially in large deformation problems. The proposed method is verified via different benchmark problems solved by commercial software. Finally, the robustness of the proposed algorithm is discussed compared to the classic methods.

In the following, in Section 2, the theory of the Large Deformation problems focusing on the continuum mechanics standpoint and FEM discretization is presented. Section 3 introduces the computational details of the proposed framework and Section 4 is dedicated to numerical examples and validation. Finally, Section 5 concludes the results and the paper's idea.

[DOI: 10.22068/ijoce.2024.14.1.579]

2. EXPERIMENTAL PROCEDURE

2.1 Example 1: Planar 10-bar truss example

This section is dedicated to introducing the Large Deformation Theory. In the beginning, the continuum mechanics description of the large deformation theory is proposed including the Deformation Gradient Theory, Strain Tensor, Green-Lagrange Strain, Stress Tensor, and Equilibrium Equation of a continuum body. In the following, the FEM details for large deformation are presented containing the Galerkin discretization process, strain-displacement tensor, plane condition tensor, and stiffness matrix. Finally, the solution procedure is discussed and the drawbacks of the prevalent methods such as the Newton-Raphson are clarified.

2.1.1 Continuum Mechanics Description

Consider a continuum body in equilibrium with domain Ω, boundary Γ, and normal vector $\boldsymbol{n_\Gamma}$ in which the traction $\boldsymbol{t}$ is imposed at boundary Γ_t and is prescribed by displacement $\tilde{\boldsymbol{u}}$ at boundary Γ_u. This configuration is shown in Fig. 1.

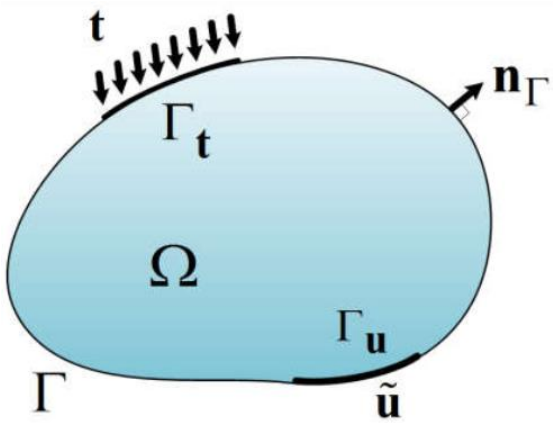

Figure 1. A continuum body in equilibrium

By considering a volume element in the initial configuration, $\boldsymbol{dX}$, it is possible to deform the continuum body using the deformation gradient as explained in Eq. 1.

$$\overrightarrow{dx} = F\overrightarrow{dX} \tag{1}$$

where **F** is the deformation gradient, and $\boldsymbol{dX}$ and $\boldsymbol{dx}$ are the volume elements in the initial and deformed configurations, respectively. Therefore, it is possible to define the deformation gradient (**F**) as Eq 2.

$$F_{ij} = \frac{\partial x_i}{\partial X_j} \tag{2}$$

where $\boldsymbol{X}$ and $\boldsymbol{x}$ represent the position of the continuum body in the initial and deformed

[DOI: 10.22068/ijoce.2024.14.1.579]

configurations, respectively. By using the concept of the deformation gradient, it is possible to define displacement vector $\boldsymbol{u}$ as Eq. 3. Fig. 2 displays the concept of the deformation gradient and displacement vector.

$$\vec{u} = \vec{x} - \vec{X} \tag{3}$$

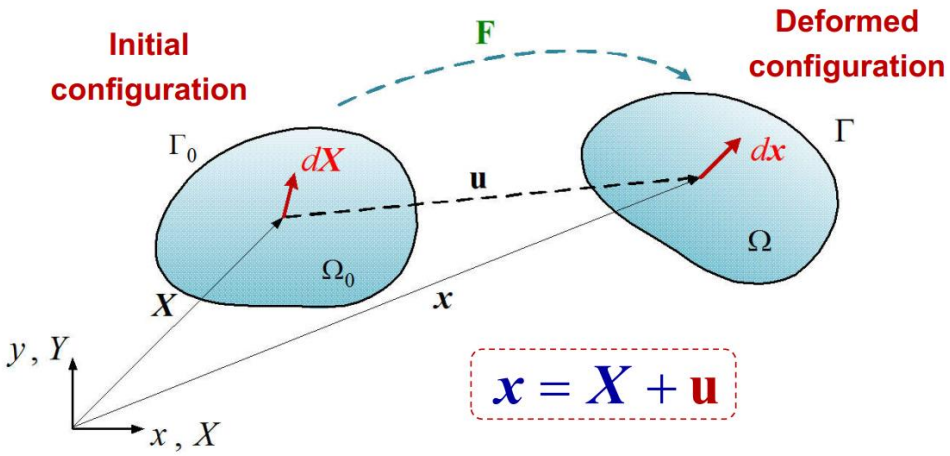

Figure 2. The initial and deformed configurations of a continuum body in equilibrium.

Based on the deformation gradient and displacement vector, it is possible to define the Green-Lagrange strain tensor as Eq. 4. This definition can capture the large deformation in continuum mechanics problems.

$$E = \frac{1}{2}(F^T F - I) \tag{4}$$

where **I** is the identity matrix. Due to the Green-Lagrange definition of the strain field, it is possible to divide the strain components into linear and nonlinear terms, as explained in Eq. 5 and Eq. 6.

$$E = E_L + E_{NL} \tag{5}$$

$$E_{ij} = \frac{1}{2}\left[\left(\frac{\partial u_i}{\partial X_j} + \frac{\partial u_j}{\partial X_i}\right) + \left(\frac{\partial u_k}{\partial X_i}\frac{\partial u_k}{\partial X_j}\right)\right] \tag{6}$$

For more details in proofs and definitions, the respected readers can refer to continuum mechanics references [29]. As described above, there are two configurations for a continuum body in equilibrium that are called the initial and deformed, respectively. One of the most important questions is when we define the stress as force per area, which area between the initial and deformed configuration should be selected as the computational one? For solving this important question, it is essential to define different types of stress. If we select the

[DOI: 10.22068/ijoce.2024.14.1.579]

geometry data from the initial configuration, then we implement the Piola-Kirchhoff stress definition. On the other hand, if we select the geometry data from the deformed configuration, then we define the Cauchy stress field. For large deformation problems, due to lack of information in the deformed configuration, the problem should be solved using Piola-Kirchhoff stress fields. An appropriate introduction to different stress fields can be found in Reddy [30].

Finally, the equilibrium equation of a continuum body can be defined as Eq. 7.

$$\frac{\partial P}{\partial X} + \vec{b} = 0 \tag{7}$$

where ***b*** is the body force vector, **P** is the second Piola-Kirchhoff stress tensor, and ***X*** is the body statements in the initial configuration. This form of the equilibrium equation is known as the strong form.

2.1.2 Nonlinear Finite Element Analysis

For a strong form equilibrium equation (Eq. 7), the weak form can be defined as Eq. 8.

$$\int_{\Omega}^{\cdot} \Delta F^T P d\Omega_0 - \int_{\Omega}^{\cdot} \Delta u^T b d\Omega_0 - \int_{\Omega}^{\cdot} \Delta u^T t d\Gamma_0 = 0 \tag{8}$$

where Δ is the Laplace operator. This weak form can be used for the Galerkin discretization process. The corresponding result is presented in Eq. 9.

$$\Psi(u) = \int B^T P d\Omega_0 - f = 0 \tag{9}$$

where **B** is the strain-displacement tensor defined as the derivatives of the shape functions and ***f*** is the problem force vector. This discretization procedure helps us to employ the concept of mesh in our analysis. Due to using mesh, it is possible to define the stiffness matrix for each element. In contrast to the linear problem, there are two different stiffness matrices for an element. The material tangent stiffness matrix and Geometric stiffness matrix are presented in Eq. 10 and Eq. 11, respectively.

$$K^{Material} = \int B^T D B d\Omega \tag{10}$$

$$K^{Geometric} = \int G^T M G d\Omega \tag{11}$$

where D is the material property matrix and G and M are defined as Eq. 12 and Eq. 13, respectively.

[DOI: 10.22068/ijoce.2024.14.1.579]

$$G = \begin{bmatrix} \frac{\partial N_i}{\partial X} & 0 \\ 0 & \frac{\partial N_i}{\partial X} \\ \frac{\partial N_i}{\partial Y} & 0 \\ 0 & \frac{\partial N_i}{\partial Y} \end{bmatrix} \tag{12}$$

$$M = \begin{bmatrix} S_{xx} I_{2\times 2} & S_{xy} I_{2\times 2} \\ S_{xy} I_{2\times 2} & S_{yy} I_{2\times 2} \end{bmatrix} \tag{13}$$

where ***N*** is element shape functions, *i* is the number of nodes within each element, ***X*** and ***Y*** are position components of the initial configuration, **S** is the second Piola-Kirchhoff stress tensor, and **I** is the identity matrix.

After the definition of the stiffness matrix, it is possible to create the system of equations for the problem, as presented in Eq. 14.

$$KU = F \tag{14}$$

where **K** is the problem total stiffness matrix, ***F*** is the total force vector, and ***U*** is the total displacement vector. In contrast to linear problems, it is impossible to solve this system of equations straightly. This is due to a lack of information from the next step or deformed configuration. It means that it is not clear for us to know from infinite possible deformations which one will be selected by the continuum body. Therefore, we should consider some additional principles such as minimum potential Energy to satisfy problem conditions. This procedure requires iterative trial-error methods to update the initial configuration to the deformed one. From this point, the most important step of a nonlinear analysis will be started. Also, this step (configuration updating) consumes more than 80 percent of the problem costs (either time or memory). Therefore, it is crucial to explain this step and know how we can handle its computational difficulties. Fig. 3 illustrates the configuration updating procedure.

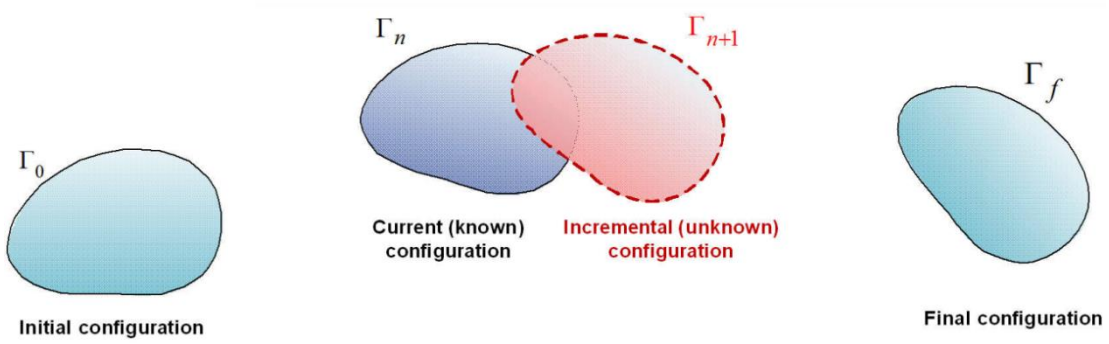

Figure 3. The configuration updating procedure.

[DOI: 10.22068/ijoce.2024.14.1.579]

Section 2.3 is dedicated to the details of the configuration updating procedure. Also, readers can refer to the nonlinear FEM references for more details and proof [31].

2.1.3 Computational and Complimentary Notes

As mentioned before, in large deformation problems, it is necessary to employ an iterative solver to obtain the results of the system of equations. For this aim, the configuration updating procedure should be implemented. Therefore, the procedure is divided into n steps in which Eq. 14 is transferred into Eq. 15.

$$K\Delta U - \Delta F = 0 \tag{15}$$

The Δ sign indicates that the procedure of the problem solving is implemented incrementally using n steps. Therefore, the configuration updating procedure can be achieved. However, as mentioned before, due to the Piola-Kirchhoff stress formulation, the nodal fields on the incremental configuration are unknown. Therefore, to obtain the correct solution it is vital to divide each step into m iterations and try to achieve the correct nodal field. This procedure is shown in Fig. 4.

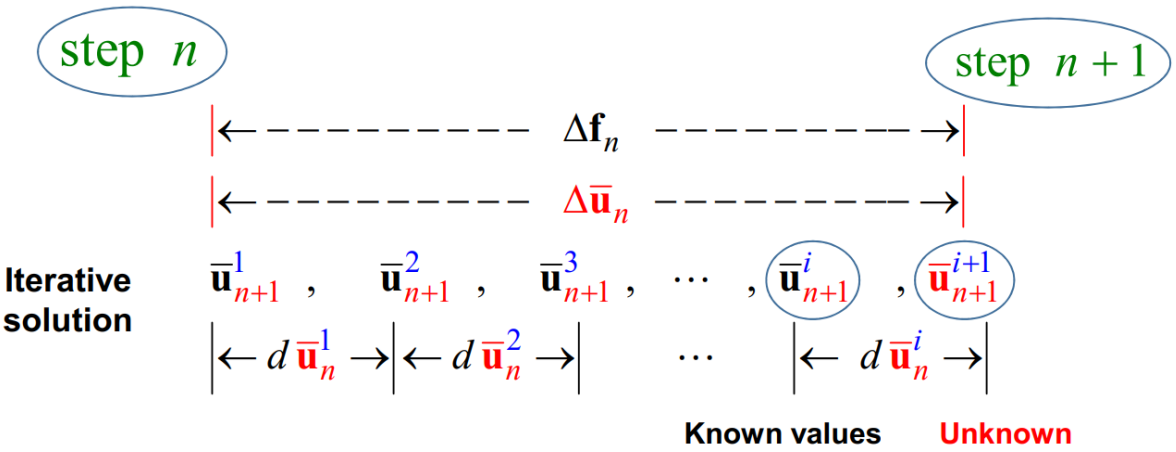

Fig. 4. Iterative procedure to obtain unknown variables between steps n and n+1.

When a nodal field is guessed, Eq. 15 has not vanished. Therefore, it is not equal to zero. The remaining values are called Residuals. Here, a solver is required to conduct the guessed nodal fields to vanish the residuals. Fig. 5 illustrates the procedure of finding the solution to a nonlinear problem.

Generally, the Newton-Raphson algorithm is used to vanish residuals. The Newton-Raphson method is categorized as a gradient-based algorithm. Therefore, there are several computational issues when the gradient behavior of the problem is not regular. It is the most important reason that several numbers of modified versions of this algorithm are developed. In this paper, a meta-heuristic algorithm is employed to vanish the problem residuals. According to the author's knowledge, the application of the meta-heuristic algorithms to the Finite Element Method (FEM) problems has introduced by Kaveh and Seddighian [21], for the first time. In this paper, this proposed framework is extended to the nonlinear problems,

[DOI: 10.22068/ijoce.2024.14.1.579]

focusing on the large deformation problems.

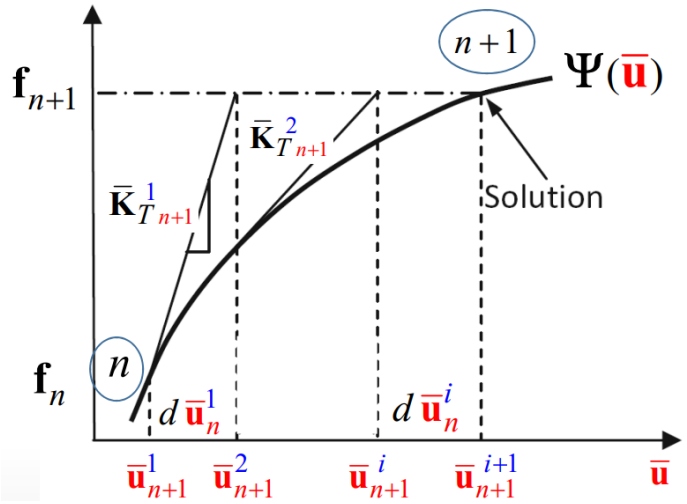

Figure 5. The iterative solution of a nonlinear problem.

2.2 Computational Algorithm

As introduced before, the main novelty of this paper is to utilize the meta-heuristic algorithms as solvers of the system of equations obtained by nonlinear FEM analysis in large deformation problems. This idea help researcher to improve some drawbacks of the gradient-based algorithms such as the Newton-Raphson method and its various modified versions. For example, in problems in which the snap-back or through-back behaviors are found, these gradient-based algorithms cannot converge. Although there are some appropriate solutions to make a nonlinear FEM problem converge, such as the Arc-Length method, these methods are difficult to implement. However, meta-heuristic algorithms are robust, easy to implement, and fast to converge to the global or near-global optimum. In the following, firstly, a brief introduction to the meta-heuristic algorithms is presented. After that, the utilized meta-heuristic algorithm in the current study is presented in detail.

2.2.1 Meta-Heuristic Algorithms

In these times, those types of computational algorithms, which are called meta-heuristics have gained wide usage in engineering, applied mathematics, economics, medicine, and other fields. The first category of meta-heuristic algorithms is the nature-inspired one. Some behavior of Animals such as migrating, hunting, flocking, and foraging procedures are very suitable for computational simulation. Therefore, these behaviors can be studied and implemented as swarm intelligent rules to develop an appropriate meta-heuristic algorithm. For instance, one of the most powerful meta-heuristic algorithms that are known as Particle Swarm Optimization or PSO is inspired by the social behavior of birds flocking or fish schooling. As another example, Water Strider Algorithm (WSA) mimics the life cycle of water strider bugs and their intelligent ripple communication. other types of meta-heuristic algorithms are developed according to the physical laws such as Black Holes Mechanics Optimization (BHMO) algorithm [32]. Also, there are some meta-heuristics based on mathematical models. The Covariance Matrix Adaptation Evolution Strategy (CMA-ES)

[DOI: 10.22068/ijoce.2024.14.1.579]

algorithm is one of them. Finally, some meta-heuristic algorithms such as Teaching-Learning Based Optimization (TLBO) algorithm are developed based on humans' behavior.

In this paper, one of the most powerful meta-heuristic algorithms, known as the Enriched Firefly Algorithm (EFA), is utilized to solve large deformation problems in continuum mechanics using the Finite Element Method (FEM). Therefore, FA and its enriched version are explained in the following.

2.2.2 Firefly Algorithm and its Enriched Version

The basic version of the Firefly algorithm (FA) was presented by Yang [33] and has been applied successfully in either continuous or discrete optimization problems. Although it is proven that FA is a better algorithm than many other optimization meta-heuristic algorithms, there are some drawbacks to its computational processes. For instance, Khadwilard et al. [34] indicated that the FA could not find the optimum solution to some problems and was trapped in the local optima. Therefore, many adaptive, hybrid, chaotic, improved, and enhanced versions of basic FA have been developed so far. One of the most complete and comprehensive reviews of the FA and its implementations can be found in.

For the implementation of the FA, there are two critical considerations. First, the variation of light intensity, and second, the formulation of attractiveness. The appropriate assumption, for simplicity, is that the attractiveness of a firefly is indicated by its brightness which is, in turn, mapped to the encoded cost function. in minimization cases, the brightness of a firefly at location $\boldsymbol{x}$ can be selected approximately as Eq. 16.

$$I(\boldsymbol{x}) \cong \frac{1}{f(\boldsymbol{x})} \tag{16}$$

where $I(\boldsymbol{x})$ is the brightness, $f(\boldsymbol{x})$ is the objective function, and $\boldsymbol{x}$ is the position vector of the firefly. Therefore, if the cost function has a higher value in this type of problem, the corresponding firefly will have less brightness. The variations of light intensity and attractiveness are monotonically reducing functions being as the light intensity and the attractiveness reduces, the distance from the source increases, and vice-versa. This procedure is formulated as Eq. 17.

$$I(r) = \frac{I_0}{1 + \gamma r^2} \tag{17}$$

where $I(r)$ is the light intensity, r is the firefly distance, and I_0 is the light intensity at the source. Since the air absorbs part of the light and makes it weaker, the air absorption is modeled mathematically by the light absorption coefficient γ. In many problems and applications, the combined effect of both can be approximated using the Gaussian form as formulated in Eq. 18.

$$I(r) = I_0 e^{-\gamma r^2} \tag{18}$$

The attractiveness of a firefly (β) is proportional to its brightness (or light intensity). β

[DOI: 10.22068/ijoce.2024.14.1.579]

can be defined as Eq. 19.

$$\beta(r) = \beta_0 e^{-\gamma r^2} \tag{19}$$

where β_0 is the attractiveness at $r = 0$. Finally, the ith firefly movement (exploration and exploitation) towards the brighter and more attractive one j is modeled using Eq. 20.

$$x_i(t) = x_i(t) + \beta_0 r^{-\gamma r_{i,j}^2}\left(x_j - x_i\right) + \alpha(rand - 0.5) \tag{20}$$

where α is the randomization parameter, *rand* is a random number uniformly distributed between *0* and *1*, and $r_{i,j}$ is the Euclidean distance between fireflies i and j.

The Enriched version of the basic Firefly Algorithm or EFA is proposed by Kaveh and his intelligent student Seddighian [35]. As they mentioned in their paper, some computational steps in the firefly algorithm increase its computational complexity of it. The first is to calculate the Euclidean distance between each pair of fireflies. The corresponding computational complexity to this process is equal to $O(N^2)$, where N is the number of fireflies. Therefore, the first enrichment is devoted to linearizing this step. There are many programming tricks to handle this drawback. The authors of the EFA paper [35] propose to define a radius ξ as Eq. 21.

$$\xi = \lambda r_{m,n} \tag{21}$$

where λ is the region coefficient corresponding to the problem type, m and n are the best and worst fireflies in each iteration, respectively. Also, λ can be decreased linearly in each iteration.

Herein, it is possible to select those fireflies that are in a feasible circular region of radius ξ in which the best firefly in each iteration is in the center. Using this trick, the algorithm's computational complexity will be converted to $T \times O(N)$, where N is the total number of fireflies, and T is the number of fireflies within the feasible region. The second change in the firefly algorithm that seems to make it more effective is to modify the position vector dimension. Each firefly position vector contains N variables, where N is the number of decision variables utilized to obtain the Euclidean distance between two fireflies. It is proposed that the corresponding value of the objective function with each firefly be added to the vector position. Therefore, each position vector includes the $N+1$ variable. This minor enrichment on the vector position improves the convergence rate of the algorithm impressively.

Finally, the last enrichment applied to the basic version of FA is to change from the Euclidean to the Mahalanobis distance. Since the deviation from the best cost is important, it is essential to consider how each variable indicates similar behavior to the best objective. This tendency can be formulated mathematically using the covariance matrix. In statistics and probability theory, covariance measures how much two random variables change together. A positive covariance means that the two variables tend to move along, while two variables move inversely if and only if their relative covariance is negative. In the case of

[DOI: 10.22068/ijoce.2024.14.1.579]

two jointly distributed real-valued random variables, the covariance of *X* and *Y* are defined by Eq. 22.

$$cov(X,Y) = E[(X - E(X)),(Y - E(Y))] \tag{22}$$

where *E(X)*, and *E(Y)* is the expected values of *X* and *Y*, respectively. The covariance matrix is a square and symmetric matrix given by Eq. 23.

$$C_{ij} = cov(X_i, X_j), C \in R^d \tag{23}$$

where *d* is the number of problem dimensions. For example, for two-dimensional problems, it can be written as Eq. 24.

$$C = \begin{bmatrix} cov(X,X) & cov(X,Y) \\ cov(Y,X) & cov(Y,Y) \end{bmatrix} \tag{24}$$

where *C* is the covariance matrix. The Mahalanobis distance is a measure of the distance between points or vectors. It can be stated that the Mahalanobis distance indicates dissimilarity measured between two vectors. The Mahalanobis distance can be formulated as Eq. 25.

$$d(\boldsymbol{x},\boldsymbol{y}) = \sqrt{(\boldsymbol{x}-\boldsymbol{y})C^{-1}(\boldsymbol{x}-\boldsymbol{y})} \tag{25}$$

where *C* is the covariance matrix between position vectors $\boldsymbol{x}$ and $\boldsymbol{y}$. If the covariance matrix is identity, then the Mahalanobis distance will be equal to the Euclidean distance. The results obtained from the mathematical benchmark functions and other structural ones indicate that the last enrichment increases the convergency rate of the algorithm efficiently.

3. NEUMERICAL SIMULATION RESULTS AND DISCUSSIONS

The introduced concepts above, are implemented in four examples. The first one is a benchmark structural analysis program in which the geometric nonlinearity can not be captured by the Newton-Raphson method. However, the proposed meta-heuristic framework can capture the nonlinear behavior of the problem entirely. In examples 2 to 4, three-dimensional problems including uniaxial, simple shear, and biaxial tests are solved using the proposed framework. For validation, the contour results of the displacement and stress fields are compared with ABAQUS commercial software. The results indicate that the proposed algorithm can capture the solution fields appropriately without loss of accuracy. Additionally, in some problems, such as example 1, in which the Newton-Raphson method can not capture the behavior, the proposed framework can be utilized successfully.

[DOI: 10.22068/ijoce.2024.14.1.579]

3.1 Example 1

One of the most famous geometric nonlinear problems in structural analysis is shown in Fig. 6.

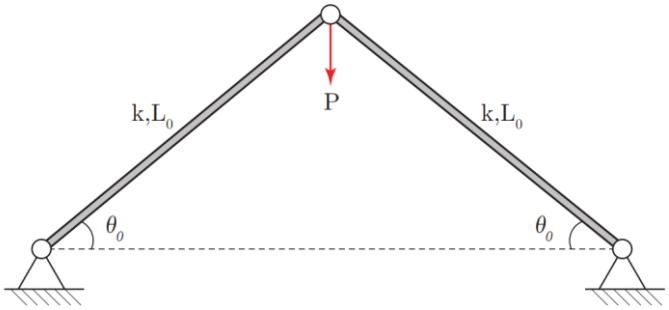

Figure 6. The configuration of the geometric nonlinearity problem.

In this problem, by increasing the Load P, the angle between bars and the horizontal line will be decreased (Fig. 7).

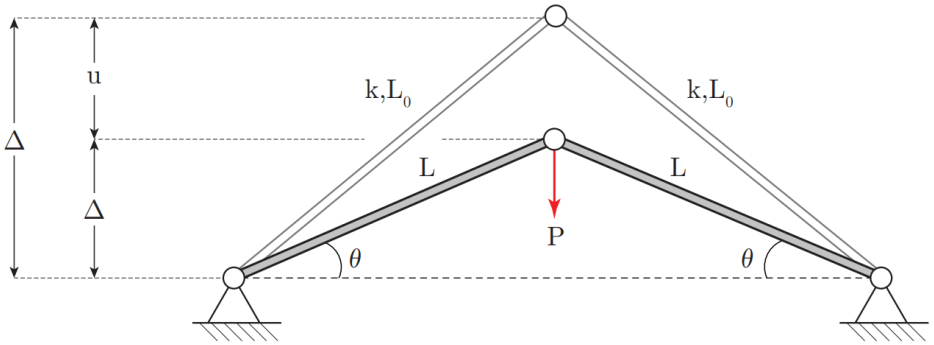

Figure 7. The behavior of the structure is due to increasing the load.

The behavior of the problem is obviously nonlinear. The exact behavior of the force-displacement curve is explained in Eq. 26 and illustrated in Fig. 8.

$$\lambda(a) = \left(\frac{1}{\sqrt{1 - 2\,\mathrm{asin}(\theta_0) + a^2}}\right)(\sin(\theta_0) - a) \tag{26}$$

where λ and a are normalized load and displacement as introduced in Eq. 27 and Eq. 28.

$$\lambda = \frac{P}{2kL_0} \tag{27}$$

$$a = \frac{u}{L_0} \tag{28}$$

where P is the nodal load, k is the bar stiffness, L_0 is the initial length of the bars, and u is the nodal displacement.

[DOI: 10.22068/ijoce.2024.14.1.579]

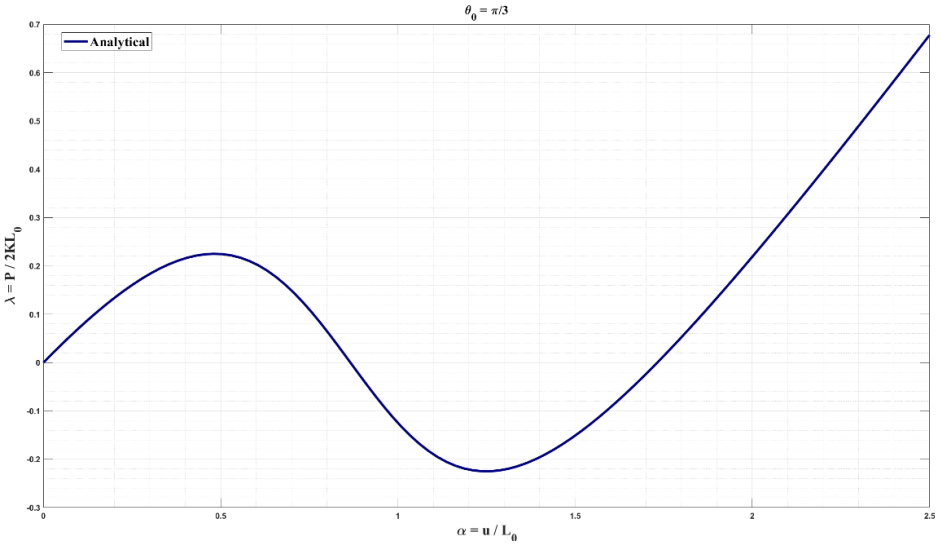

Figure 8. The exact force-displacement curve of example 1.

If the Finite Element Method (FEM) analysis has been utilized for this problem via the Newton-Raphson method, it is impossible to capture the entire behavior of the structure. The corresponding results to this analysis and its comparison with the analytical solution are shown in Fig. 9.

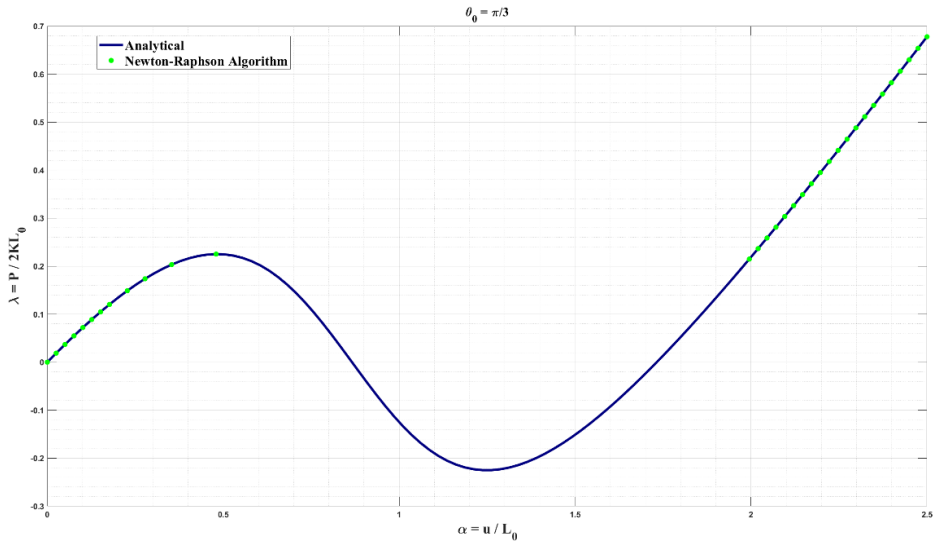

Figure 9. The comparison between analytical and the Newton-Raphson method solutions.

In contrast to the Newton-Raphson method, the proposed framework in this paper can capture the entire behavior of this structure. The comparison of the proposed framework with the analytical solution and the Newton-Raphson method is plotted in Fig. 10 and Fig. 11, respectively.

[DOI: 10.22068/ijoce.2024.14.1.579]

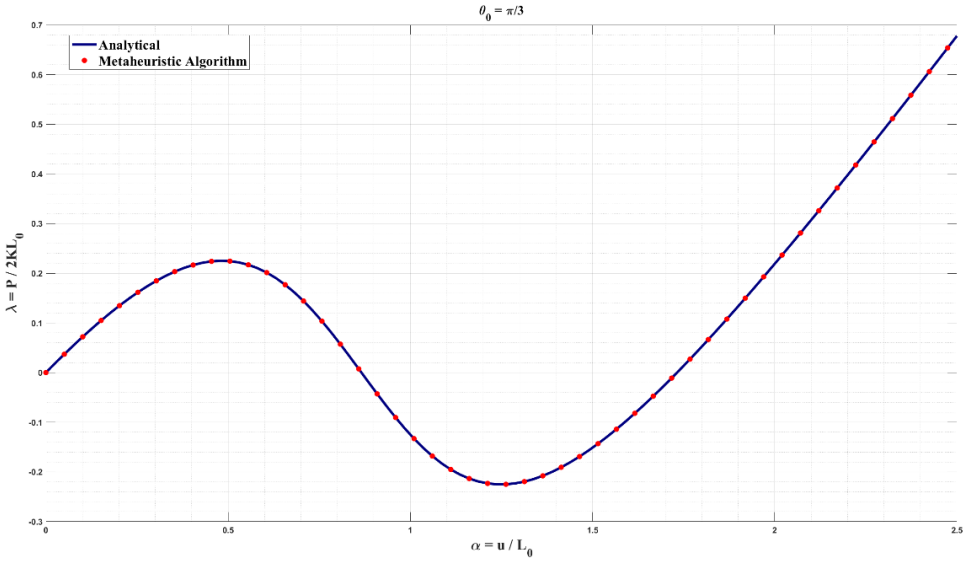

Figure 10. The comparison between analytical and the proposed method solutions.

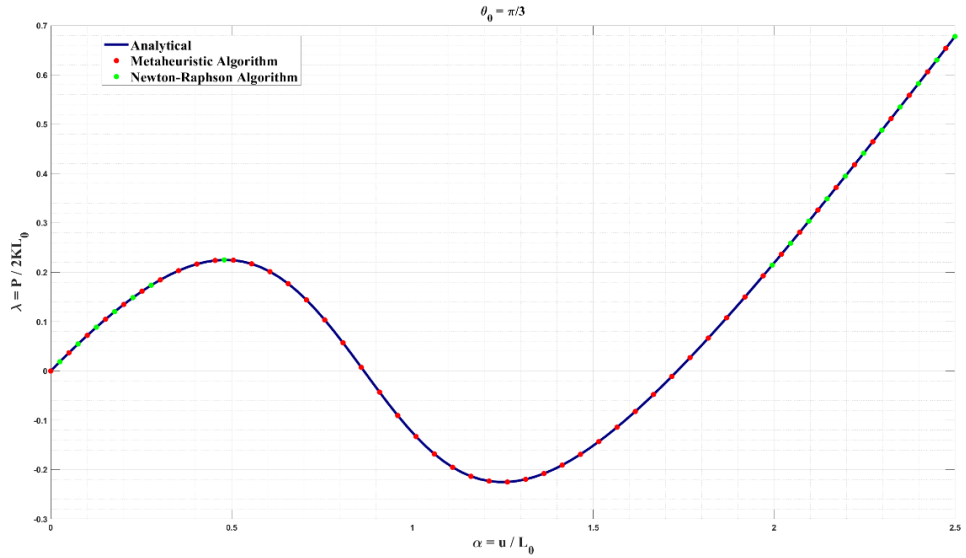

Figure 11. The comparison between analytical, the Newton-Raphson method, and proposed framework solutions.

It is obvious that the proposed meta-heuristic framework can achieve the accurate and appropriate field of the problem without any limitations. In the following, the robustness of the proposed algorithm is investigated by considering three-dimensional problems.

3.2 Example 2

Example 2 includes a uniaxial test investigated by either the proposed framework or ABAQUS commercial software. The main aim of this example is to compare the accuracy of the results obtained by the new framework with the prevalent method. In this example,

[DOI: 10.22068/ijoce.2024.14.1.579]

the size of a three-dimensional cubic is considered as 1. The material is considered steel and the box is prescribed at x-direction with 50 percent of its initial length. All units are in SI. The displacement and stress fields of both ABAQUS and the proposed method are compared for validation in Figs 12 to 15.

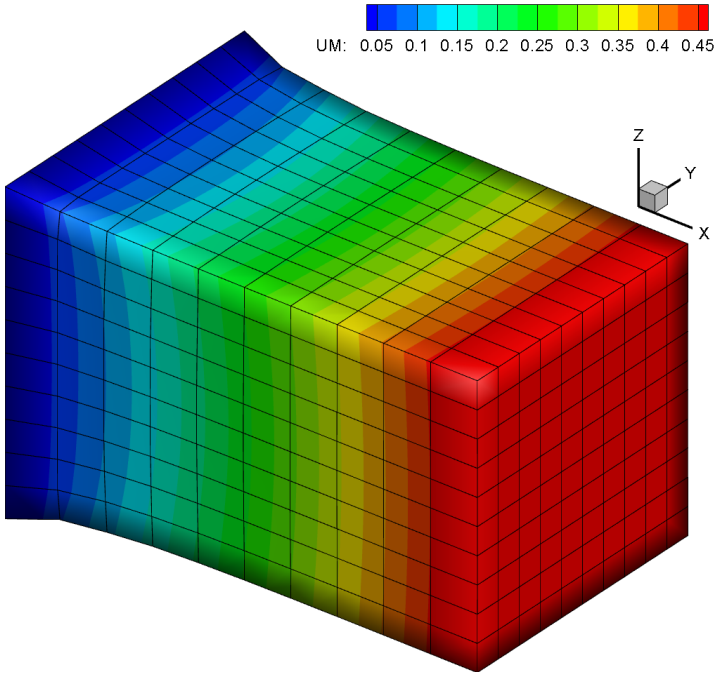

Figure 12. The magnitude displacement field of the proposed framework.

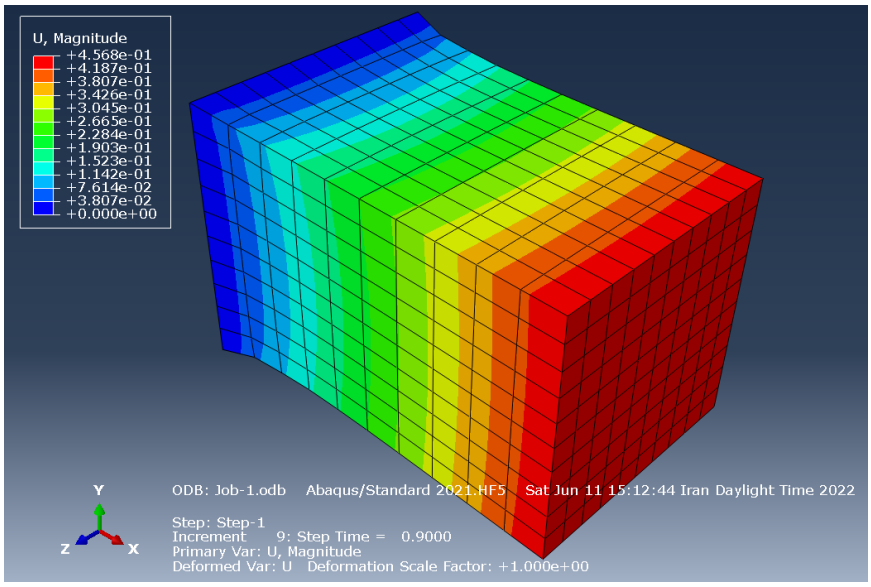

Figure 13. The magnitude displacement field of the ABAQUS.

[DOI: 10.22068/ijoce.2024.14.1.579]

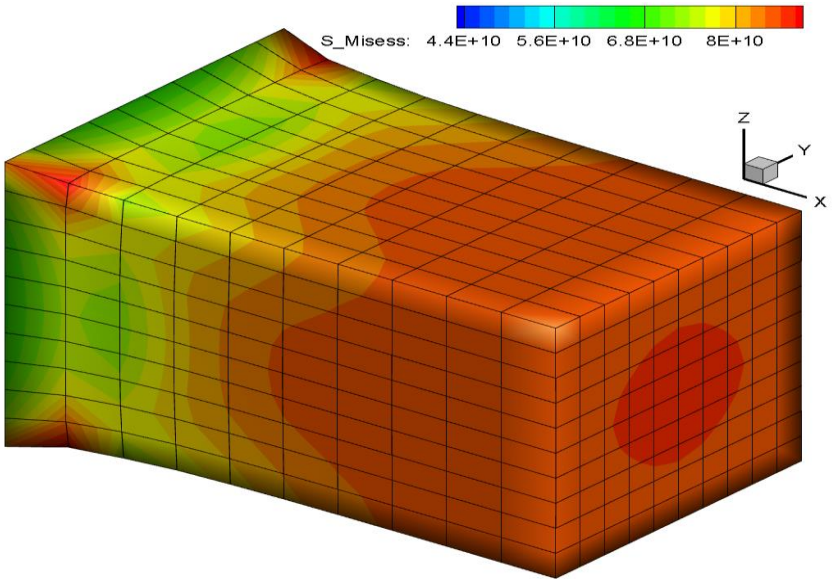

Figure 14. The von-misses stress field of the proposed framework.

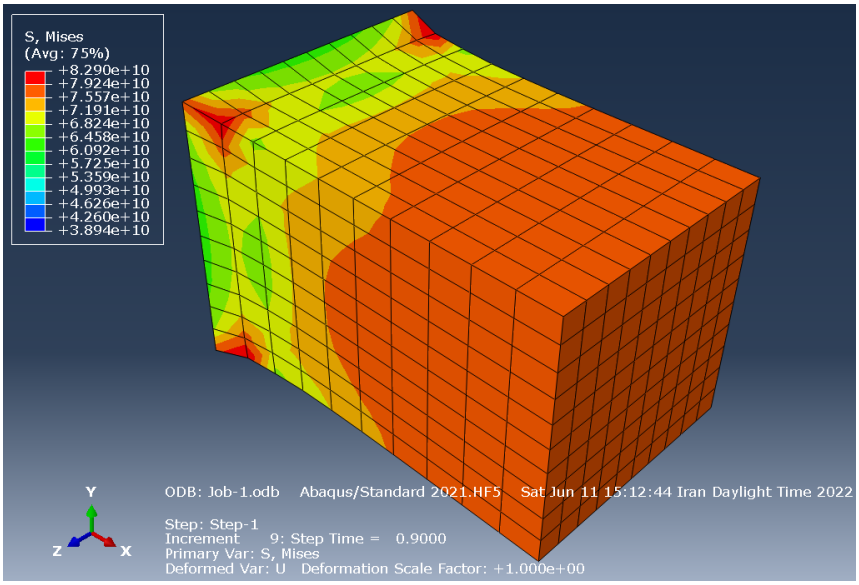

Figure 15. The von-misess stress field of the ABAQUS.

It is obvious that the results are compatible. Therefore, we can utilize the proposed framework in this paper confidently. All projects and results will be available on request.

3.3 Example 3

This example considers the shear behavior of the introduced cube in Example 2. The *XY* plane is imposed by shear deformation equal to 50 percent of its initial length. The results are compared in Figs 16 to 19.

[DOI: 10.22068/ijoce.2024.14.1.579]

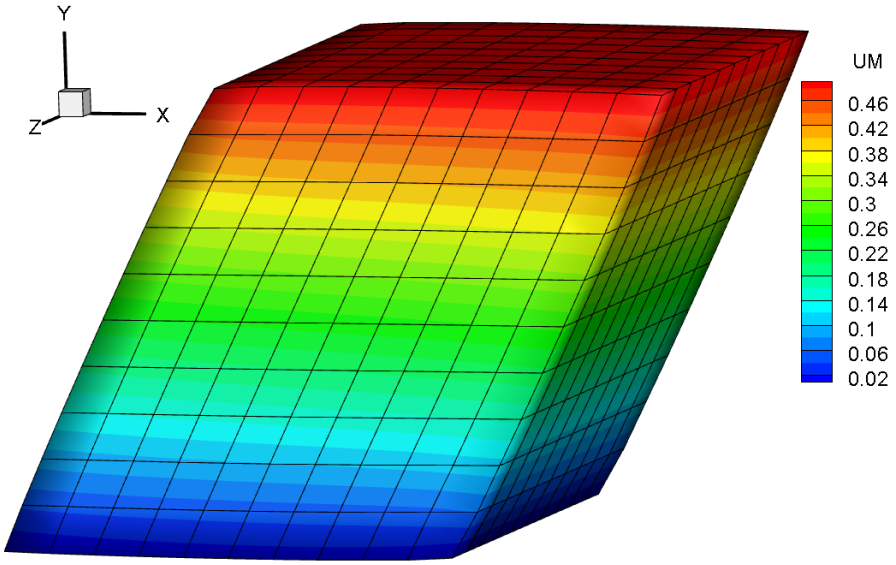

Figure 16. The magnitude displacement field of the proposed framework.

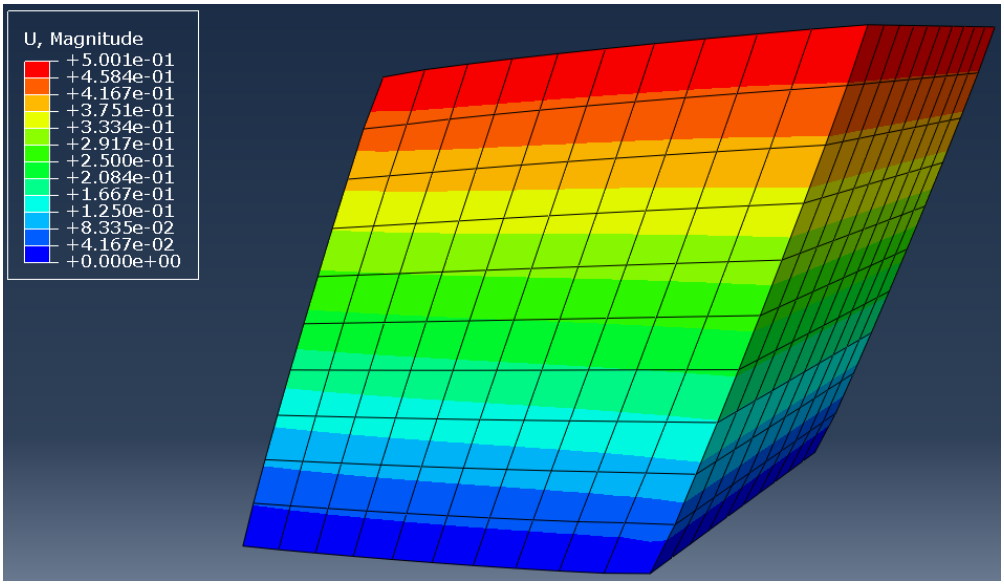

Figure 17. The magnitude displacement field of the ABAQUS.

[DOI: 10.22068/ijoce.2024.14.1.579]

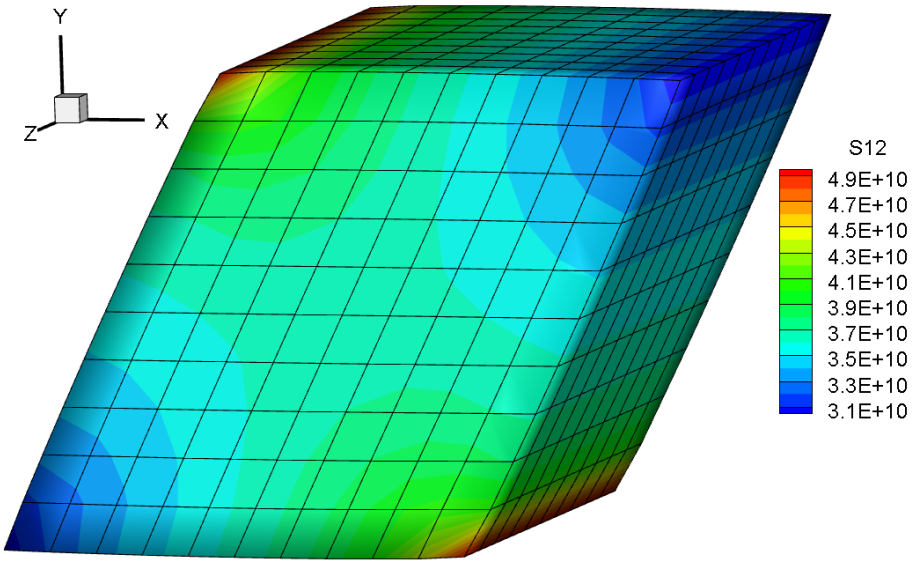

Figure 18. The shear stress field of the proposed framework.

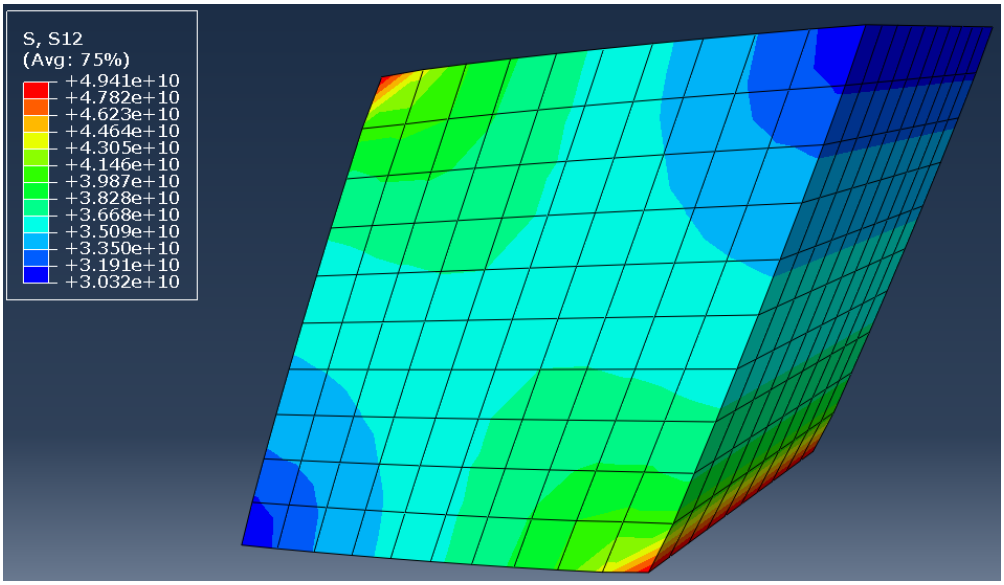

Figure 19. The shear stress field of the ABAQUS.

Similar to Example 2, the results are completely compatible. Therefore, t is possible to claim that the proposed framework in this paper is valid for either uniaxial or simple shear tests. All projects and results will be available on request.

3.4 Example 4

The last example, contains a biaxial test on the introduced cube in Examples 2 and 3, with a central hole with a radius equal to 0.2 meters. Since the problem includes the stress intensity concepts, it is more challenging to validate. The compared results are reported in Figs 20 to

[DOI: 10.22068/ijoce.2024.14.1.579]

23.

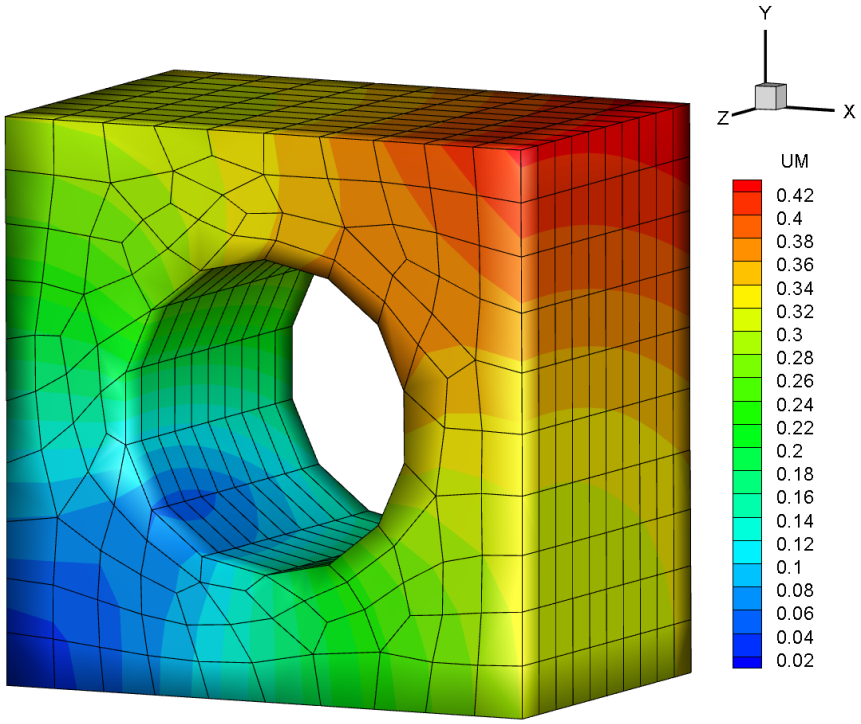

Figure 20. The magnitude displacement field of the proposed framework.

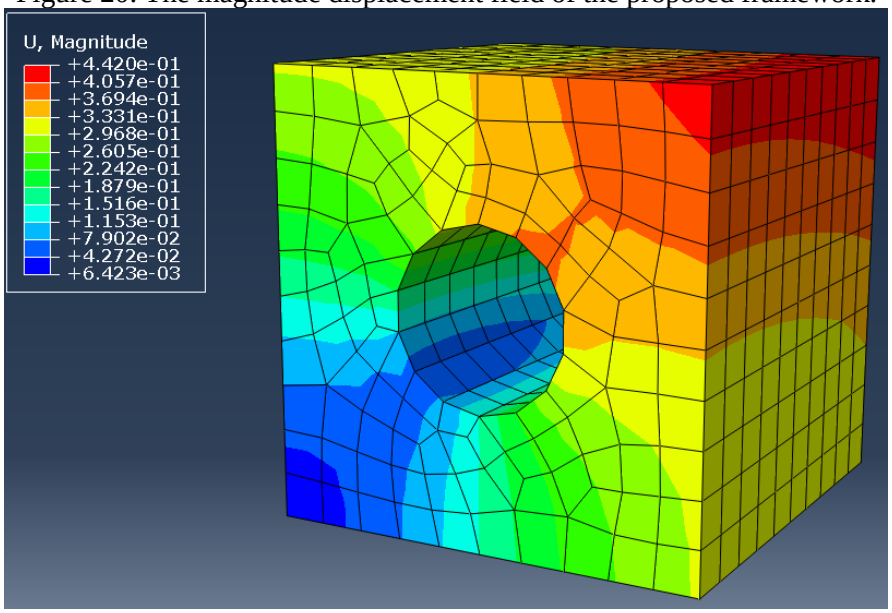

Figure 21. The magnitude displacement field of the ABAQUS.

[DOI: 10.22068/ijoce.2024.14.1.579]

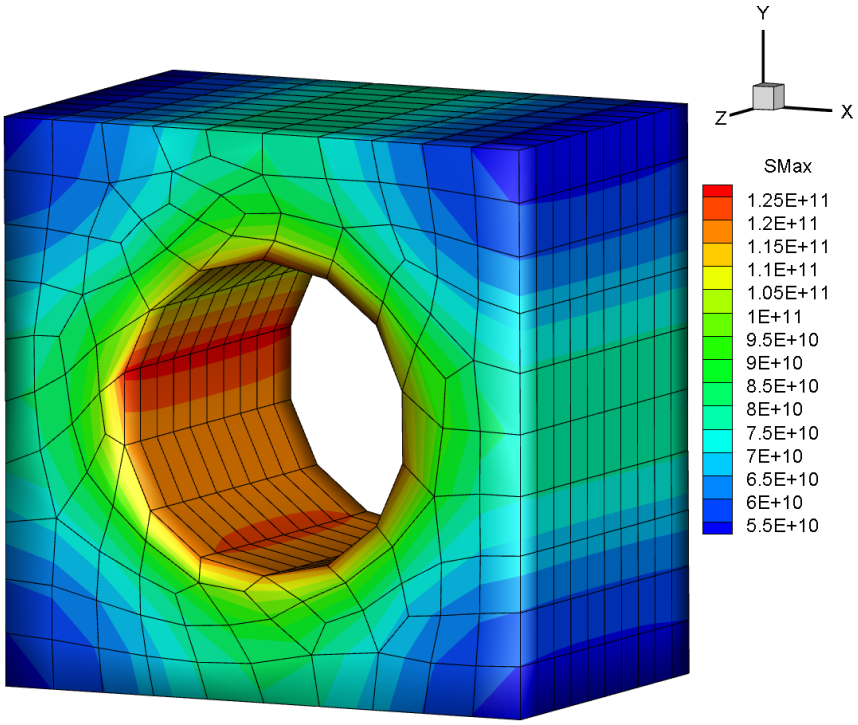

Figure 22. The maximum stress field of the proposed framework.

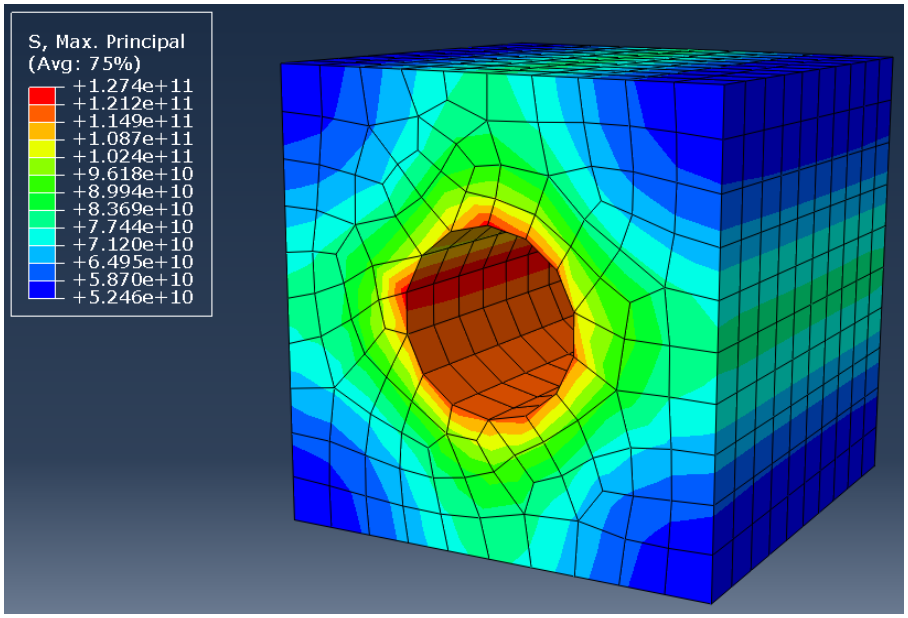

Figure 23. The maximum stress field of the ABAQUS.

Due to the compatibility of the results of the current example, now, it is possible to claim that the proposed framework can be used as an alternative approach to solving nonlinear large deformation problems using the Finite Element Method (FEM). Because it is valid for

[DOI: 10.22068/ijoce.2024.14.1.579]

different types of well-known problems (Examples 2 to 4) and is robust in solving challenging problems (Examples 1 and 4).

4. CONCLUSIONS

In this paper, a new computational framework based on a meta-heuristic algorithm has been proposed to solve any large deformation problem in continuum mechanics using the finite element method. The current framework improves the drawbacks of the computational algorithms in the FEM such as the Newton-Raphson method and its various modified versions. Also, the new method is absolutely easy to implement. Therefore, it is an appropriate alternative for methods such as arc-length that are robust but difficult to implement. For validation, firstly, a geometric nonlinear problem in structural analysis is solved and it has proved that the Newton-Raphson method cannot capture the behavior of the structure. However, the proposed method can model the problem entirely. The validity of the solutions is has obtained by comparing the results with the analytical solution. After that, the well-known problems, i.e., three-dimensional uniaxial, simple shear, and biaxial with central hole are considered either the proposed method or ABAQUS commercial software. All results indicate that the proposed framework is accurate and compatible with prevalent ABAQUS analysis results. Therefore, it is possible to claim that this new framework can be utilized as an alternative in FEM analysis, especially in large deformation problems.

REFERENCES

1. Kaveh A. *Advances in Metaheuristic algorithms for optimal design of structures*, Springer, 3th edition, Switzerland, 2021.
2. Zienkiewicz OC, Taylor RL. *The finite element method: solid mechanics*, vol. 2. Butterworth-heinemann, 2000.
3. Kaveh A, Roosta GR. Comparative study of finite element nodal ordering methods, *Eng Struct*, 1998; **20**(1–2):86–96.
4. Kaveh A, Sharafi P. Nodal ordering for bandwidth reduction using ant system algorithm, *Eng Comput*, 2009; **26**(3): 313-323.
5. Kaveh A. Ordering for bandwidth reduction, *Comput Struct*, 1986; **24**(3): 413–420.
6. Lozac'h N, Goodson AL, Powell WH. Nodal nomenclature–general principles, Angew. *Chem Int Ed Engl*, 1979; **18**(12): 887–899.
7. Polton DJ. A new method of nodal numbering for cyclic and acyclic structures, J *Chem Inf Comput Sci*, 1992; 32(5): 430–436.
8. Mohseni A, Moslemi H, Seddighian MR. An improved nodal ordering for reducing the bandwidth in FEM, *J Serb Soc Comput Mech*, 2018; 12(1): 126–143.
9. Kaveh A, Seddighian MR. Domain decomposition of finite element models utilizing eight meta-heuristic algorithms: A comparative study, *Mech Based Des Struct Mach*, pp. 1–19, 2020.
10. Kaveh A, Bondarabady HAR. A hybrid graph-genetic method for domain decomposition, *Finite Elem Anal Des*, 2003; **39**(13): 1237–47.

[DOI: 10.22068/ijoce.2024.14.1.579]

11. Kaveh A, Shojaee S. Optimal domain decomposition via p-median methodology using ACO and hybrid ACGA, *Finite Elem Anal Des*, 2008; **44**(8): 505–512.
12. Kaveh A, Seddighian MR, Hassani P. Automatic domain decomposition in finite element method–a comparative study, *Period Polytech Civ Eng*, 2022; 66(2): 323–334.
13. Chan TF, Mathew TP. Domain decomposition algorithms," Acta numerica, vol. 3, pp. 61–143, 1994.
14. Smith BF. *Domain decomposition methods for partial differential equations," in Parallel Numerical Algorithms*, Springer, 1997.
15. Dolean V, Jolivet, Nataf F. *An introduction to domain decomposition methods: algorithms, theory, and parallel implementation*. SIAM, 2015.
16. Kaveh A, Roosta GR. Domain decomposition for finite element analysis, *Commun Num Meth Eng*, 1997; **13**(2): 61–71.
17. Peters G, Wilkinson JH. On the stability of Gauss-Jordan elimination with pivoting," *Commun ACM*, 1975; **18**(1): 20–24.
18. Setiadji BH, Indriastuti AK. The use of gauss-jordan elimination method in determining the proportion of aggregate gradation, *in Proceedings of the Second International Conference of Construction, Infrastructure, and Materials*, 2022, pp. 431–440.
19. Stanimirović PS, Petković MD. Gauss–Jordan elimination method for computing outer inverses, *App Math Comput*, 2013; **219**(9): 4667–79.
20. Melab N, Talbi EG, Petiton S. A parallel adaptive Gauss-Jordan algorithm, *J Supercomput*, 2000; **17**(2): 167–185.
21. Diep DN, Giang DH, Van Minh N. Quantum Gauss-Jordan elimination and simulation of accounting principles on quantum computers, *Int J Theor Phys*, 2017; **56**(6): 1948–60.
22. Kaveh A, Seddighian MR. A new nodal stress recovery technique in finite element method using colliding bodies optimization algorithm, *Period Polytech Civ Eng*, 2019; **63**(4): 1159–70.
23. Khoei AR, Moslemi H, Seddighian MR. An efficient stress recovery technique in adaptive finite element method using artificial neural network," *Eng Fract Mech*, 2020; **237**: 107231.
24. Kaveh A, Seddighian MR, Sadeghi H, Sadat Naseri S. Optimal solution of richards'equation for slope instability analysis using an integrated enhanced version of black hole mechanics into the FEM. *Int J Opt Civ Eng*, 2020; **10**(4): 629–650.
25. Kaveh, Seddighian MR, Ghanadpour E. Upper and lower bounds for the collapse load factor of rectangular grids using FEM," *Int J Opt Civ Eng*, 2019; **9**(3): 543–554.
26. Kaveh A, Seddighian MR. Optimization of slope critical surfaces considering seepage and seismic effects using finite element method and five meta-heuristic algorithms, *Period Polytech Civ Eng*, 2021; **65**(2): 425–436.
27. Djedoui N, Ounis A. Optimization of TMD parameters in frequency domain including SSI effect by means of recent metaheuristic algorithms, *Pract Period Struct Des Constr*, 2022;. **27**(3): 04022026.
28. Tran VQ. Hybrid gradient boosting with meta-heuristic algorithms prediction of unconfined compressive strength of stabilized soil based on initial soil properties, mix design and effective compaction, *J Clean Product*, 2022; **355**: 131683.

[DOI: 10.22068/ijoce.2024.14.1.579]

29. Ghani S, Kumari S. Liquefaction behavior of Indo-Gangetic region using novel metaheuristic optimization algorithms coupled with artificial neural network, *Nat Haz*, 2022; **111**(3): 1–35.
30. Lai WH, Rubin DH, Rubin D, Krempl E. *Introduction to continuum mechanics*, Butterworth-Heinemann, 2009.
31. Reddy JN. *An introduction to continuum mechanics*, Cambridge university press, 2013.
32. Reddy JN. *An Introduction to Nonlinear Finite Element Analysis Second Edition: with applications to heat transfer, fluid mechanics, and solid mechanics*, OUP Oxford, 2014.
33. Kaveh A, Seddighian MR, Ghanadpour E. Black Hole Mechanics Optimization: a novel meta-heuristic algorithm, *Asian J Civ Eng*, 2020; **21**(7): 1129–49.
34. Yang XS, Slowik A. *Firefly algorithm, in Swarm Intelligence Algorithms*, CRC Press, 2020.
35. Khadwilard A, Chansombat S, Thepphakorn T, Chainate W, Pongcharoen P. Application of firefly algorithm and its parameter setting for job shop scheduling, *J Ind Tech*, 2012; **8**(1): 49–58.
36. Kaveh A, Seddighian MR. Simultaneously multi-material layout, and connectivity optimization of truss structures via an Enriched Firefly Algorithm, *Structures*, 2020; **27**: 2217–31.

[DOI: 10.22068/ijoce.2024.14.1.579]